

The pressure-temperature phase diagram of URu₂Si₂ under hydrostatic conditions

Nicholas P. Butch,¹ Jason R. Jeffries,² William J. Evans,² Songxue Chi,³ Juscelino B. Leão,³ Jeffrey W. Lynn,³ Stanislav V. Sinogeikin,⁴ James J. Hamlin,⁵ Diego A. Zocco,⁵ and M. Brian Maple⁵

¹Center for Nanophysics and Advanced Materials, Department of Physics, University of Maryland, College Park, MD 20742, USA

²Condensed Matter and Materials Division, Lawrence Livermore National Laboratory, Livermore, CA 94550, USA

³NIST Center for Neutron Research, Gaithersburg, MD 20899, USA

⁴HPCAT, Advanced Photon Source, Argonne National Laboratory, Argonne, IL 60439, USA

⁵Department of Physics, University of California, San Diego, La Jolla, CA 92093, USA

ABSTRACT

The pressure dependence of the hidden order phase of the heavy fermion superconductor URu₂Si₂ has been a subject of intense research since shortly after the discovery of the compound decades ago. Applied pressure increases the critical temperature of the paramagnetic / hidden order transition and brings about a transition to long-range antiferromagnetism. The reported pressures and temperatures of these phase boundaries vary between studies: 4 – 7 kbar at low temperature and 12 – 15 kbar at high temperature. We review experimental evidence that the measured values of pressure and temperature are very sensitive to the chosen pressure transmitting medium. Recent x-ray diffraction measurements suggest that the relative position of the silicon atom in the unit cell is changing as a function of pressure. Recent neutron diffraction measurements show that the zero-temperature limit of the hidden order / antiferromagnetic transition occurs at pressures greater than 7.5 kbar.

INTRODUCTION

The moderately heavy fermion superconductor URu₂Si₂ is notorious for its hidden order (HO) phase, whose order parameter remains unidentified. The transition from a heavy paramagnetic state into the HO phase at approximately 17 K [1-3] is characterized by a large BCS-like specific heat anomaly [1], anomalies in ultrasound [4] and thermal expansion [5], a substantial increase in thermal conductivity [6], a hump in electrical resistivity [1], a kink in magnetic susceptibility [1], the opening of a large gap in the incommensurate spin excitation spectrum [7], the crossing of the chemical potential by a heavy electron band [8], and a small seemingly extrinsic strain-induced magnetic moment [9,10]. These phenomena point to a partial gapping of the Fermi surface at the transition into the HO state. While the existence of a small dipole moment, too small to account for the entropy released at the transition, has long been an associated mystery, it is becoming accepted that this small moment appears due to residual strain in samples. In the absence of a large dipole moment, it has been theoretically necessary to invoke exotic ordering of either local or itinerant electrons as the underlying cause. Many theories describing the HO parameter have been suggested over the years; recent proposals include nesting-driven [11,12] and unconventional Kondo scenarios [13].

URu₂Si₂ has been studied under high magnetic field, applied pressure, and chemical substitution. The critical field of the HO phase is about 36 T, and in its vicinity 5 different phases have been identified [14]. Chemical substitution on the transition metal site suppresses the HO, but in the case of Re substitution, ferromagnetic order is stabilized [15-17]. The ferromagnetism is associated with non-Fermi liquid behavior [18], unconventional critical magnetic scaling exponents [19], and energy-temperature scaling in the dynamic susceptibility [20]. A comparison of the resulting phase diagram to that obtained from the substitution of Rh is available in Reference [21].

Current understanding of the effects of pressure on URu₂Si₂ has a long history. It was known early on that the HO transition temperature T_0 increases under applied hydrostatic pressure [22–25] and that the slope increases substantially at a critical pressure of about 12 kbar [25–29]. In contrast, superconductivity is suppressed. The small ambient pressure moment grows by an order of magnitude under pressure, giving rise to long range antiferromagnetic (AFM) order at 15 kbar [30]. However, the moment does not grow continuously. Rather, the HO and AFM states coexist heterogeneously below 15 kbar, as indicated by NMR [31,32] and μ SR measurements [33,34]. These studies established a zero temperature critical pressure of about 5 kbar, generally consistent with measurements of dilation under pressure [35]. Magnetic susceptibility measurements suggested that superconductivity does not coexist with AFM [36] which was confirmed by neutron scattering and ac susceptibility [37]. The authors identified a critical pressure of 7 kbar, but revised this value to 5-6 kbar in a later study [38]. The overall phase diagram was corroborated by measurements of electrical resistivity and ac calorimetry performed on the same sample [39], and has been now been extended by measurements in magnetic field [40]. Recent neutron Larmor diffraction measurements are in agreement as well [41].

The anisotropic effects of uniaxial stress have also been studied. Stress applied along the a -axis suppresses superconductivity and enhances HO, while stress applied along the c -axis does the opposite [42,43]. This is consistent with the fact that the AFM moment increases only when stress is applied along the basal plane [44].

However, not all experiments fit the mold nicely. The de Haas–van Alphen effect appears insensitive to the HO–AFM transition [45]. The very high-magnetic-field phase diagram shows little change under pressure [46]. Moreover, the superconductivity has also been observed to persist to pressures significantly greater than 5 kbar in magnetization [47] and electrical resistivity measurements [48,49].

These examples, the sensitivity of URu₂Si₂ to anisotropic stress, along with the significant scatter in determined values of critical pressure, inspired us to take a closer look at the experimental conditions under which such pressure measurements are made. We report on recent pressure studies on URu₂Si₂. First, we review evidence that shows that the transition into the HO state is very sensitive to the hydrostaticity of the pressure medium used [50]. Next, we describe preliminary x-ray diffraction measurements under pressure that indicate a pressure-induced change in the relative positions of Si atoms [51]. Finally, we briefly discuss neutron diffraction measurements under pressure using a helium cell under the most hydrostatic conditions available, where we find that the HO-AFM transition actually occurs at pressures greater than 7.5 kbar [52], in excess of values reported to date. Our results highlight the sensitivity of these much-studied phase transitions to experimental conditions.

EXPERIMENT

Single crystals of URu₂Si₂ were grown via the Czochralski technique in electrical tri-arc and tetra-arc furnaces, followed by a 900 °C anneal in Ar for one week in the presence of a Zr getter. Crystals were oriented via x-ray Laue back reflection or single crystal x-ray diffraction, and samples were cut via spark erosion or wire saw.

Measurements of electrical resistivity ρ as a function of T and P were performed using BeCu piston-cylinder cells in a pumped ⁴He cryostat. To ensure hydrostatic pressure environments in a fluid medium up to 30 kbar, a 1:1 volume mixture of n-pentane / isoamyl alcohol was used. In addition, two kinds of commonly used liquid fluorinated hydrocarbon, Fluorinert FC75 and a 1:1 volume mixture of FC70/FC77, were used to establish the degree to which measurements of ρ on URu₂Si₂ are sensitive to non-hydrostatic conditions. The superconducting transition of Pb was used as a manometer.

X-ray diffraction measurements under pressure were performed on powdered samples in membrane-driven diamond anvil cells (DACs) using Ar as a pressure medium and the R1 fluorescence line of ruby chips for manometry. Pressure gradients in the cell remained less than 1 kbar. The DACs were cooled using a liquid helium flow cryostat. Angle-dispersive x-ray diffraction measurements were performed in transmission using a 33.6 keV (0.03694 nm) incident x-ray beam at the HPCAT beamline 16 ID-B of the Advanced Photon Source at Argonne National Laboratory.

Neutron diffraction measurements under pressure were performed at the NIST Center for Neutron Research on the BT-9 triple axis spectrometer with 14.7 meV incident energy. A 1 g single crystal was placed into an Al-alloy He-gas pressure cell that was cooled using a closed cycle refrigerator. The pressure cell was connected to a pressurizing intensifier through a heated high-pressure capillary. Pressure was adjusted only at temperatures well above the helium melting curve and the capillary was heated during slow cooling of the cell to accommodate the contracting He gas, minimizing pressure loss.

RESULTS & DISCUSSION

Liquid pressure media

A comparison of the pressure dependence of T_0 , defined as the local resistive minimum, determined via measurements of $\rho(T)$ in various pressure media, is presented in Figure 1. We first discuss 1:1 n-pentane/isoamyl alcohol, as these measurements are reversible and reflect the most hydrostatic environment. The main feature is a discontinuous change in slope at 15 kbar, associated with the transition from HO to long-range AFM. Note that there is no difference in the data whether increasing or decreasing P , which follows from the fact that the room-temperature hydrostatic limit of 1:1 n-pentane/isoamyl alcohol is at least 30 kbar [53], a value exceeding the pressure range here. The phase boundary determined from measurements in FC70/FC77 is superficially similar, although the high pressure slope is small by comparison and the kink at 15 kbar upon pressurization is much less pronounced. The data on depressurization instead have a gentle S shape, and a fit with two straight lines to the data below 20 kbar yields an intersection in the vicinity of 7–8 kbar. These values can be explained by the loss of hydrostaticity at about 8 kbar [54]. Measurements in FC75 yield a visibly different phase boundary. Initially, the

pressurization curves closely match those from the measurement in 1:1 n-pentane/isoamyl alcohol and a sharp kink is visible at 15 kbar. However, upon depressurization there is dramatic hysteresis. Eventually the initial pressurization curve is recovered at 12 kbar, which corresponds to the hydrostatic limit of FC75 [54]. Once pressure is increased again, the data appear to fall on a second, parallel line. However, the line is shifted downward in pressure, indicating the persistence of residual shear stresses. Despite its nominally higher hydrostatic limit relative to FC70/FC77, the hysteresis observed in FC75 is much more pronounced, which suggests that these limits are not directly indicative of how strong pressure hysteresis effects will be once the hydrostatic limit is exceeded. These measurements also demonstrate that it is possible to produce an incorrect, although seemingly reasonable, phase boundary if great care is not taken.

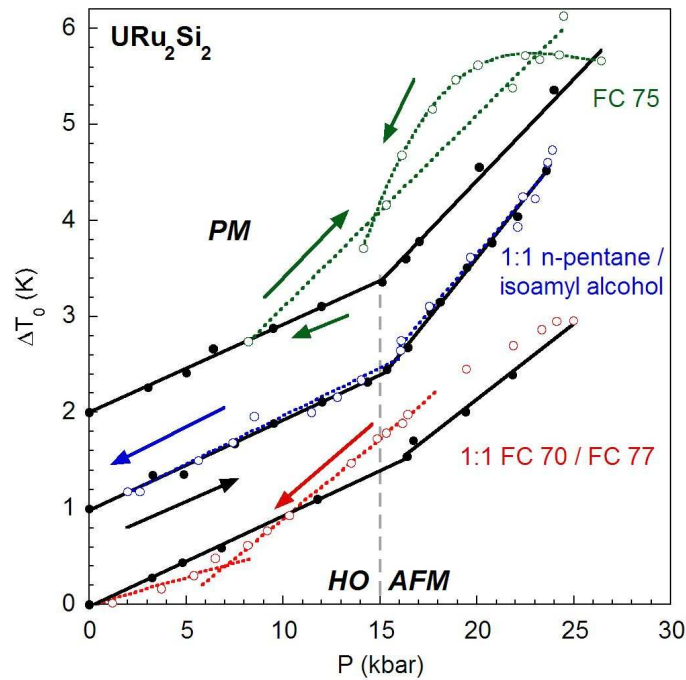


Figure 1. Phase boundary between PM and HO/AFM phases (T_0) as determined in different pressure-transmitting media. Filled data points were taken during pressurization, open data points during de-pressurization. Using a 1:1 mixture of n-pentane/isoamyl alcohol, there is no hysteresis. Using a 1:1 mixture of FC70/FC77, the high pressure slope is reduced and hysteresis is evident upon depressurization. Using FC75, significant hysteresis is observed upon depressurization and re-pressurization.

X-ray diffraction

In the ThCr_2Si_2 crystal structure, the Si atoms occupy sites with a free z -parameter, which allows them to shift relative position within the unit cell without altering the crystal structure or symmetry. Variations in the z -coordinate change the relative intensity of the Bragg reflections. At ambient pressure, the z -coordinate is reported to be $z = 0.3710$ [55]. The positions of the Si atoms within the URu_2Si_2 crystal structure are shown in Figure 2 as a function of T and P . The z -coordinate changes little with T for both pressures shown here. For both pressures, the calculated

values stay within approximately 0.2% of those means from 6 – 30 K and it appears that the positions of the Si atoms in the lattice are not strongly affected by the onset of the HO or AFM states. However, with increasing pressure, the value of z at 6 K decreases. The change in the z coordinate of the Si site results in a flattening of the Ru-Si cage surrounding the U ions and significant changes in bond lengths. A contraction of the Ru-Si bond length compresses the Ru-Si layers vertically, while the large change in the Si-Si next nearest neighbor bond length leads to decreased bonding between Ru-Si layers across U atoms. Because these two effects create a more two-dimensional structure, they may play a role in the HO-AFM transition. Efforts to clarify this scenario are underway [51].

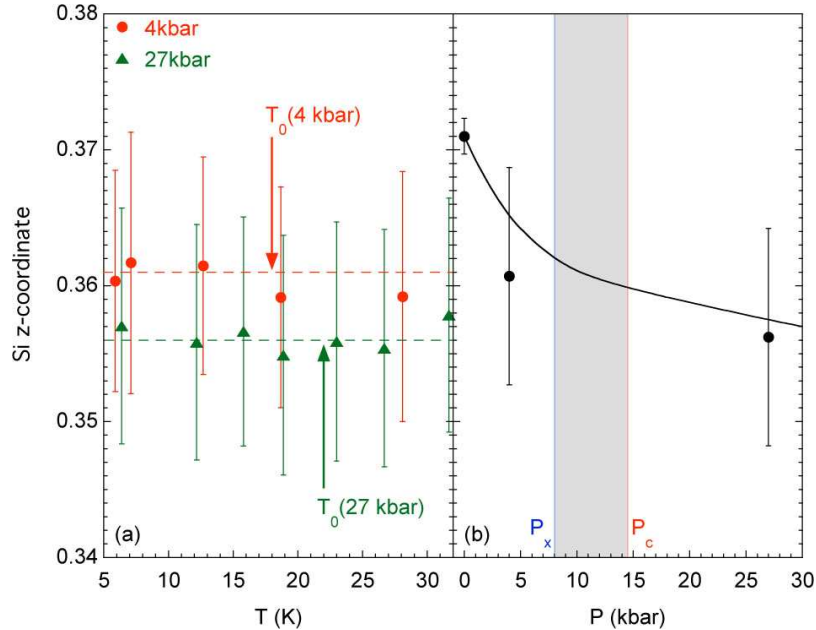


Figure 2. Relative z -coordinate of Si within the lattice. a) Temperature dependence at 4 kbar and 27 kbar. The lines represent the mean values of z for each pressure, and the HO or AFM transitions are denoted by the arrows. (b) Pressure dependence at 6 K. The grey rectangle represents the approximate range over which HO evolves toward AFM with increasing temperature and pressure. The solid line is a guide to the eye. Error bars are returned from structural refinement.

Neutron diffraction

Preliminary results of neutron diffraction measurements are discussed next. Inspired by an earlier study of Bourdarot and coworkers that showed no AFM moment up to 5 kbar in a helium cell [56] and the wide range of variation in reported values of the phase boundary between HO and AFM phases, we investigated the onset of AFM order in the most hydrostatic medium available, using a He cell with a maximum working pressure of 10 kbar. In order to study the onset of AFM order, the experiment focused on the (100) peak, which is a forbidden nuclear reflection and thus clearly establishes the existence of an AFM moment. Normalized rocking scans at 1.5 K are shown in Figure 3. The ambient pressure moment for this sample is smaller than $0.02 \mu_B$. While some magnetic diffraction is readily apparent already at 7.6 kbar, the most rapid increase in moment occurs between 8.0 and 8.6 kbar. This rapid increase as a function

of pressure at constant temperature is indicative of a first-order transition and is consistent with the discontinuous increase of the moment as a function of temperature at constant pressures greater than 8 kbar (not shown). A more complete report of this measurement and a detailed analysis, along with a comparison to resistivity data, will be presented in an upcoming manuscript [52].

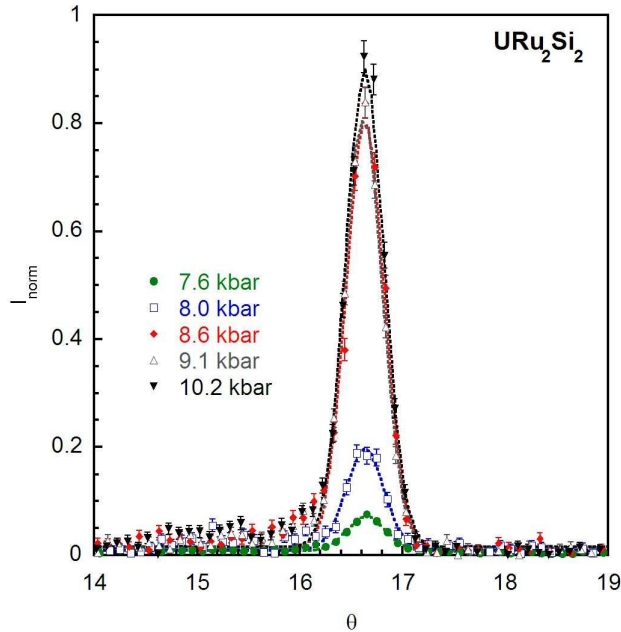


Figure 3. Neutron diffraction rocking scans about the magnetic 100 peak at 1.5 K measured at different pressures. The abrupt growth of the moment with pressure is consistent with a first-order transition to an AFM ground state. Uncertainties are statistical and represent one standard deviation.

CONCLUSIONS

The pressure dependence of the HO phase has been shown to be very sensitive to the experimental conditions under which it is measured. The resistive anomaly associated with the HO transition displays varying degrees of hysteresis depending on the pressure transmitting medium. Preliminary x-ray diffraction measurements suggest that while the lattice parameters do not change dramatically under pressure, there may be an internal rearrangement of atoms. Neutron diffraction measurements show that the HO-AFM transition is also very sensitive to environment. When using a helium pressure transmitting medium the zero-temperature critical pressure is greater 7.5 kbar, far in excess of most published values.

ACKNOWLEDGMENTS

NPB is supported by a CNAM Glover Fellowship. JRJ and WJE are supported by the Science Campaign at Lawrence Livermore National Laboratory. JJH, DAZ, and MBM are supported by the National Nuclear Security Administration under the Stewardship Science

Academic Alliance program through the U.S. Department of Energy under Grant No. DE-FG52-06NA26205. Sample synthesis was supported by the U.S. Department of Energy under Research Grant DE-FG-02-04ER46105. Lawrence Livermore National Laboratory is operated by Lawrence Livermore National Security, LLC, for the U.S. Department of Energy, National Nuclear Security Administration under Contract DE-AC52-07NA27344. Portions of this work were performed at HPCAT (Sector 16), Advanced Photon Source (APS), Argonne National Laboratory. HPCAT is supported by DOE-BES, DOE-NNSA, NSF, and the W.M. Keck Foundation. APS is supported by DOE-BES, under Contract No. DE-AC02-06CH11357. The identification of any commercial product or trade name does not imply endorsement or recommendation by the National Institute of Standards and Technology.

REFERENCES

1. M. B. Maple, J. Chen, Y. Dalichaouch, T. Kohara, C. Rossel, M. S. Torikachvili, M. W. McElfresh, and J. D. Thompson, *Phys. Rev. Lett.* **56**, 185 (1986).
2. T. T. M. Palstra, A. A. Menovsky, J. van den Berg, A. J. Dirkmaat, P. H. Kes, G. J. Nieuwenhuys, and J. A. Mydosh, *Phys. Rev. Lett.* **55**, 2727 (1985).
3. W. Schlabitz, J. Baumann, B. Pollit, U. Rauchschalbe, H. M. Mayer, U. Ahlheim, and C. D. Bredl, *Z. Phys. B* **62**, 171 (1986).
4. K. Kuwahara, H. Amitsuka, T. Sakakibara, O. Suzuki, S. Nakamura, T. Goto, M. Mihalik, A. A. Menovsky, A. de Visser, and J. J. M. Franse, *J. Phys. Soc. Jpn.* **66**, 3251 (1997).
5. A. de Visser, F. E. Kayzel, A. A. Menovksy, J. J. M. Franse, J. van den Berg, and G. J. Nieuwenhuys, *Phys. Rev. B* **34**, 8168 (1986).
6. P. A. Sharma, N. Harrison, M. Jaime, Y. S. Oh, K. H. Kim, C. D. Batista, H. Amitsuka, and J. A. Mydosh, *Phys. Rev. Lett.* **97**, 156401 (2006).
7. C. R. Wiebe, J. A. Janik, G. J. MacDougall, G. M. Luke, J. D. Garrett, H. D. Zhou, Y.-J. Jo, L. Balicas, Y. Qiu, J. R. D. Copley, Z. Yamani, and W. J. L. Buyers, *Nat. Phys.* **3**, 96 (2007).
8. A. F. Santander-Syro, M. Klein, F. L. Boariu, A. Nuber, Pascal Lejay, and Friedrich Reinert, *Nat. Phys.* **5**, 637 (2009).
9. C. Broholm, J. K. Kjems, W. J. L. Buyers, P. Matthews, T. T. M. Palstra, A. A. Menovsky, and J. A. Mydosh, *Phys. Rev. Lett.* **58**, 1467 (1987).
10. H. Amitsuka, K. Matsuda, I. Kawasaki, K. Tenya, M. Yokoyama, C. Sekine, N. Tateiwa, T.C. Kobayashi, S. Kawarazaki, and H. Yoshizawa, *J. Magn. Magn. Mater.* **310**, 214 (2007).
11. S. Elgazzar, J. Ruzs, M. Amft, P. M. Oppeneer, and J. A. Mydosh, *Nat. Mat.* **8**, 337 (2009).
12. A. V. Balatsky, A. Chantis, Hari P. Dahal, David Parker, and J. X. Zhu, *Phys. Rev. B* **79**, 214413 (2009).
13. K. Haule and G. Kotliar, *Nat. Phys.* **5**, 796 (2009).
14. K. H. Kim, N. Harrison, M. Jaime, G. S. Boebinger, and J. A. Mydosh, *Phys. Rev. Lett.* **91**, 256401 (2003).
15. Y. Dalichaouch, M. B. Maple, M. S. Torikachvili, and A. L. Giorgi, *Phys. Rev. B* **39**, 2423 (1989).
16. Y. Dalichaouch, M. B. Maple, R. P. Guertin, M. V. Kuric, M. S. Torikachvili, and A. L. Giorgi, *Physica B* **163**, 113 (1990).
17. Y. Dalichaouch, M. B. Maple, J. W. Chen, T. Kohara, C. Rossel, M. S. Torikachvili, and A. L. Giorgi, *Phys. Rev. B* **41**, 1829 (1990).

18. E. D. Bauer, V. S. Zapf, P.-C. Ho, N. P. Butch, E. J. Freeman, C. Sirvent, and M. B. Maple, *Phys. Rev. Lett.* **94**, 046401 (2005).
19. N. P. Butch and M. B. Maple, *Phys. Rev. Lett.* **103**, 076404 (2009).
20. V. V. Krishnamurthy, D. T. Adroja, N. P. Butch, S. K. Sinha, M. B. Maple, R. Osborn, J. L. Robertson, S. E. Nagler, and M. C. Aronson, *Phys. Rev. B* **78**, 024413 (2008).
21. N. P. Butch and M. B. Maple, *J. Phys.: Condens. Matter* **22**, 164204 (2010).
22. F. R. de Boer, J. J. M. Franse, E. Louis, A. A. Menovsky, J. A. Mydosh, T. T. M. Palstra, U. Rauchschwalbe, W. Schlabitz, F. Steglich, and A. de Visser, *Physica* **138B**, 1 (1986).
23. E. Louis, A. de Visser, A. Menovsky, and J. J. M. Franse, *Physica* **144B**, 48 (1986).
24. Y. Onuki, T. Yamazaki, I. Ukon, T. Omi, K. Shibusaki, T. Komatsubara, I. Sakamoto, Y. Sugiyama, R. Onodera, K. Yonemitsu, A. Umezawa, W. K. Kwok, G. W. Crabtree, and D. G. Hinks, *Physica* **148B**, 29 (1987).
25. R. A. Fisher, S. Kim, Y. Wu, N. E. Phillips, M. W. McElfresh, M. S. Torikachvili, and M. B. Maple, *Physica B* **163**, 419 (1990).
26. M. W. McElfresh, J. D. Thompson, J. O. Willis, M. B. Maple, T. Kohara, and M. S. Torikachvili, *Phys. Rev. B* **35**, 43 (1987).
27. Y. Uwatoko, K. Iki, G. Oomi, Y. Onuki, and T. Komatsubara, *Physica B* **177**, 147 (1992).
28. M. Ido, Y. Segawa, H. Amitsuka, and Y. Miyako, *J. Phys. Soc. Jpn.* **62**, 2692 (1993).
29. J. P. Brison, N. Keller, P. Lejay, A. Huxley, L. Schmidt, A. Buzdin, N. R. Bernhoeft, I. Mineev, A. N. Stepanov, J. Flouquet, D. Jaccard, S. R. Julian, and G. G. Lonzarich, *Physica B* **199&200**, 70 (1994).
30. H. Amitsuka, M. Sato, N. Metoki, M. Yokoyama, K. Kuwahara, T. Sakakibara, H. Morimoto, S. Kawarazaki, Y. Miyako, and J. A. Mydosh, *Phys. Rev. Lett.* **83**, 5114 (1999).
31. K. Matsuda, Y. Kohori, T. Kohara, K. Kuwahara, and H. Amitsuka, *Phys. Rev. Lett.* **87**, 087203 (2001).
32. K. Matsuda, Y. Kohori, T. Kohara, H. Amitsuka, K. Kuwahara, and T. Matsumoto, *J. Phys.: Condens. Matter* **15**, 2363 (2003).
33. H. Amitsuka, K. Tenya, M. Yokoyama, A. Schenck, D. Andreica, F. N. Gygax, A. Amato, Y. Miyako, Y. K. Huang, and J. A. Mydosh, *Physica B* **326**, 418 (2003).
34. A. Amato, M. J. Graf, A. de Visser, H. Amitsuka, D. Andreica, and A. Schenck, *J. Phys.: Condens. Matter* **16**, S4403 (2004).
35. G. Motoyama, T. Nishioka, and N. K. Sato, *Phys. Rev. Lett.* **90**, 166402 (2003).
36. S. Uemura, G. Motoyama, Y. Oda, T. Nishioka, and N. K. Sato, *J. Phys. Soc. Jpn.* **74**, 267 (2005).
37. H. Amitsuka, K. Matsuda, I. Kawasaki, K. Tenya, M. Yokoyama, C. Sekine, N. Tateiwa, T. C. Kobayashi, S. Kawarazaki, and H. Yoshizawa, *J. Magn. Mater.* **310**, 214 (2007).
38. H. Amitsuka, K. Matsuda, M. Yokoyama, I. Kawasaki, S. Takayama, Y. Ishihara, K. Tenya, N. Tateiwa, T. C. Kobayashi, and H. Yoshizawa, *Physica B* **403**, 925 (2008).
39. E. Hassinger, G. Knebel, K. Izawa, P. Lejay, B. Salce, and J. Flouquet, *Phys. Rev. B* **77**, 115117 (2008).
40. D. Aoki, F. Bourdarot, E. Hassinger, G. Knebel, A. Miyake, S. Raymond, V. Taufour, and J. Flouquet, *J. Phys. Soc. Jpn.* **78**, 053701 (2009).
41. P. G. Niklowitz, C. Pfleiderer, S. Mühlbauer, P. Böni, T. Keller, P. Link, J. A. Wilson, M. Vojta, and J. A. Mydosh, *Physica B* **404**, 2955 (2009).
42. K. Bakker, A. de Visser, E. Brück, A. A. Menovsky, and J. J. M. Franse, *J. Magn. Mater.* **108**, 63 (1992).

43. A. Guillaume, B. Salce, J. Flouquet, and P. Lejay, *Physica B* **259-261**, 652 (1999).
44. M. Yokoyama, H. Amitsuka, K. Tenya, K. Watanabe, S. Kawarazaki, H. Yoshizawa, and J. A. Mydosh, *Phys. Rev. B* **72**, 214419 (2005).
45. M. Nakashima, H. Ohkuni, Y. Inada, R. Settai, Y. Haga, E. Yamamoto, and Y. Onuki, *J. Phys.: Condens. Matter* **15**, S2011 (2003).
46. Y. J. Jo, L. Balicas, C. Capan, K. Behnia, P. Lejay, J. Flouquet, J. A. Mydosh, and P. Schlottmann, *Phys. Rev. Lett.* **98**, 166404 (2007).
47. K. Tenya, I. Kawasaki, K. Tameyasu, S. Yasuda, M. Yokoyama, H. Amitsuka, N. Tateiwa, and T.C. Kobayashi, *Physica B* **359-361**, 1135 (2005).
48. J. R. Jeffries, N. P. Butch, B. T. Yukich, and M. B. Maple, *Phys. Rev. Lett.* **99**, 217207 (2007).
49. J. R. Jeffries, N. P. Butch, B. T. Yukich, and M. B. Maple, *J. Phys.: Condens. Matter* **20**, 095225 (2008).
50. N. P. Butch, J. R. Jeffries, D. A. Zocco, and M. B. Maple, *High Pressure Res.* **29**, 335 (2009).
51. J. R. Jeffries, N. P. Butch, J. J. Hamlin, S. V. Sinogeikin, W. J. Evans, and M. B. Maple, in preparation.
52. N. P. Butch, J. R. Jeffries, S. X. Chi, J. B. Leao, J. W. Lynn, and M. B. Maple, in preparation.
53. A. Jayaraman, A. R. Hutson, J. H. McFee, A. S. Coriell, and R. G. Maines, *Rev. Sci. Instrum.* **38**, 44 (1967).
54. V. A. Sidorov and R. A. Sadykov, *J. Phys.: Condens. Matter* **17**, S3005 (2005).
55. G. Cordier, E. Czech, H. Schafer, and P. Woll, *J. Less-Common Met.* **110**, 327 (1985).
56. F. Bourdarot, A. Bombardi, P. Burllet, M. Enderle, J. Flouquet, P. Lejay, N. Kernavanois, V. P. Mineev, L. Paolasini, M. E. Zhitomirsky, and B. Fåk, *Physica B* **359-361**, 986 (2005).